Polish Journal of Chemical Technology, 14, 2, 42 — 48, 10.2478/v10026-012-0069-2

Heterogeneous photocatalytic removal and reaction kinetics of Rhodamine-B dye with Au loaded TiO_2 nanohybrid catalysts

Dongfang Zhang

Huazhong Agricultural University, College of Science, Hubei 430070, PR China
**Corresponding author: e-mail: zjzappletree@126.com*

Heterogeneous photocatalytic removal of Rhodamine-B (RhB) dye by metallic Au nanopatrticles deposited TiO_2 photocatalyst was studied. For this study, a chemical reduction method by hydrazine hydrate for gold deposition was employed in order to synthesize Au/TiO_2 nanocomposite system. For the characterization of the synthesized nanomaterials, X-ray diffraction (XRD), transmission electron microscopy (TEM), UV-vis diffuse reflectance spectroscopy (DRS), the Fourier transformation infrared spectroscopy (FTIR) and photoluminescence spectroscopy (PLS) techniques were performed. The obtained results show that the deposition of gold onto TiO_2 surface could effectively inhibit the recombination of the photoinduced electron and holes, improving the absorption capability for the visible light source and leading to the increased surface OH group density. The degradation experiment reveals that the efficiency of color removal from RhB aqueous solution containing Au/TiO_2 powders for the photocatalytic bleaching of RhB dye is more efficient than that of bare TiO_2 sample upon UV-vis light activation. In addition, degradation kinetics of RhB dye in aqueous suspensions can be well simulated by the Langmuir-Hinshelwood model and obeys the pseudo-first order law, with a decolorization rate of 0.0252 min^{-1} to the photocatalytic removal of RhB dye.

Keywords: Au/TiO_2 catalyst, Rhodamine-B, Decompose kinetics.

INTRODUCTION

Large amounts of dyes are annually produced and applied in different industries including textile, cosmetic, paper, leather, pharmaceutical and nutrition industries. A substantial amount of dyestuff is discharged in the textile industry, for instance, there are more than 100,000 commercially available dyes with an estimation of the annual production of over 70,000 tons, 15% of which is lost during the dyeing process[1]. The presence of even trace concentration of dyes in the effluent is highly visible and undesirable. It causes some serious problems to aquatic life and human health disorders. With the increase in the environmental awareness all over the world, search for new cost effective and green routes to treat wastewater containing dyes has increased in recent years. These concerns have led to new and strict regulations concerning colored wastewater discharge as well as developing more efficient treatment technologies.

Advanced oxidation processes (AOPs) are promising methods for the complete mineralization of organic dye[2]. AOPs include photocatalysis systems such as combination of a semiconductor material and UV light, which usually involve a heterogeneous photocatalytic process to give an excellent pathway to treat the colored water and to make it harmless. Nowadays, photocatalysis has been exploited for various environmental processes such as deodorization, water purification, air purification, sterilization and soil proof. Many researchers have have concentrated on degradation and mineralization of variety of toxic substances such as azo dyes by photocatalytic oxidation. Different types of semiconductors were used as the photocatalyst. Among these titania is the widely used photocatalyst due to its strong oxidizing power, stable at different pH, favorable band gap energy and nontoxicity to mediate the difficult-to-remove pollutants. Even though titania is the widely used semiconductor with some positive merits, it still has some disadvantage like low surface area, fast recombination and wavelength maximum lies in UV region. Since the high rate of recombination between photo-induced electron-hole pairs is a major rate-determination factor controlling the photocatalytic activity of titania, various surface modification methods have been adopted to facilitate the charge carrier move. Numerous works have concentrated on enhancing the quantum efficiency of TiO_2, for instance, by doping, metal deposition, formulating multi-junction or coupled systems[3–5]. According to the previous work, it has been already understood that doping of titana with other metal ions raises many problems. It induces the recombination sites in the bandgap, which causes the recombination of the excited electron and the hole, leading to poor photocatalytic activity. Therefore, doping is not the best method to inhibit charge carriers recombination since it is well known that dopants are often recombination centers. Doping is useful for the activation of titania towards visible light, but often these photocatalyst show much a lower photoactivity under UV. Therefore, for the higher photoactivity (lower recombination), surface modification is recommended instead of doping. It has been shown that noble metal deposition can markedly improve the photocatalytic efficiency of titania[6,7], and metal islands deposited on the semiconductor surface have been found to act as a sink for photo-induced electrons and thus the free hole in the valence band can successively participate in the oxidation reaction. In view of these, the noble metals deposited on TiO_2 act as electron trapping agents so that the life time of the excitons created can be increased, facilitating electron-hole separation and promoting the interfacial electron transfer process.

This paper deals with photocatalytic decoloration of Rhodamine-B dye on gold metallized titania nanoparticles and tries to relate their physico-chemical properties with their photocatalytic activities. The surface modification

of titania with gold was presented in this work in order to enhance the surface properties and photoactivities of bare titania. The prepared samples were characterized by XRD, TEM, UV-vis DRS, FTIR and PL spectra. The effects of the loaded gold nanoparticles on the chemical composition, crystal structure, surface states, optical properties and charge separation characteristics of pristine TiO_2 were investigated. At last, the photocatalytic activity of the Au/TiO_2 composite system was evaluated by measuring the rate of the photodegradation reaction of Rhodamine-B (RhB). The photodegradation kinetics and reaction mechanism over this nanocomposite system has also been proposed and discussed.

EXPERIMENTAL SECTION

All the reagents were purchased from Shanghai Chemicals Co. Ltd. with analytic grade and used as received without further purification. Distilled water was employed throughout in all experiments. For the synthesis of Au/TiO_2 nanocomposite, tetrabutyl titaniate ($Ti(OBu)_4$, TBOT) and $HAuCl_4{\cdot}4H_2O$ were used as titanium and gold sources, respectively. Chemical reduction of gold was carried out by using hydrazine hydrate as a reducing agent. In a typical synthesis, 10 mL of TBOT was added dropwise to 90 mL ethanol under vigorously stirring at ambient temperature (AT), named solution A. Another mixture solution consists of 120 mL distilled water (as hydrolysis agent) and a certain amount of $HAuCl_4{\cdot}4H_2O$ (29.5 mg) named solution B. The solution B was added to the solution A in terms of the nominal contents of deposited Au of 1.0% weight total to titania under vigorous stirring. Then, hydrazine hydrate solutions (6 mL $N_2H_4{\cdot}H_2O$/30 mL distilled water) was added to achieve chemical reduction of Au^{3+} ions. After aging for 24 h, the sols transformed into wet gels. Next, the white precipitate was obtained by centrifugation, followed by washing with distilled water and anhydrous ethanol for several times. After that, the wet-gel precursor was heated in an oven to evaporate the excess solvent at 80°C for 8–10 h. At last, the dried precipitate or xerogel precursor was calcined at 420°C for 3 h to get the Au/TiO_2 nanocomposite (1.0 wt.% Au/TiO_2) and ensure good adhesion of Au nanoparticles onto the TiO_2 substrate. A reference TiO_2 sol-gel sample was also prepared similarly to the method described above. The nanoparticles thus synthesized were then used for further experimental exploration, i.e., the photoactivity test.

The X-ray powder diffraction (XRD) data were recorded at room temperature with an X-ray diffractometer (XRD-6000, Shimadzu Corporation) using Cu Kα irradiation (λ = 0.15408 nm), operated at 40 kV and 100 mA, which was used to establish the crystallographic information such as structure properties, chemical composition and phases. Transmission electron microscopy (TEM, JEOL, JEM-2010, Japan) was used to observe the surface state and structure of the photocatalyst composites at an acceleration voltage of 200 kV. The percentage of UV-vis reflectance was measured by diffuse reflectance spectroscopy (DRS) for the powder form of the catalysts using a scanning UV-vis-NIR spectrophotometer (Varian Cary 500) in the region of 200–800 nm. The spectrophotometer was equipped with an integrating sphere assembly and polytetrafluoroethylene was used as a reflectance material. In situ FT-IR spectra are recorded on a Thermo Nicolet 330 FT-IR spectrometer (AVATAR) at a solution of 4.0 cm^{-1}. For each recording of IR spectra, the quantity of KBr equal, and the concentration of sample was controlled at 2 wt% of the KBr pellet. The photoluminescence (PL) emission spectra of the samples were measured with a RF-5301 PC spectrofluorophotometer (Shimadzu Corporation) by using the 320 nm line of a Xe lamp as excitation source at room temperature.

Photocatalytic efficiency of the as-prepared systems was estimated in terms of the degradation of Rhodamine-B (RhB) aqueous solution. Rhodamine-B (RhB), a xanthene dye, is widely used as a colorant in textiles and food stuffs, and also a well-known water tracer fluorescent. RhB is harmful if swallowed by human beings and animals, and causes irritation to the skin, eyes and respiratory tract. The carcinogenicity, reproductive and developmental toxicity, neurotoxicity and chronic toxicity towards humans and animals have been experimentally proven[8]. The artificial light photocatalytic activity test is conducted in a quartz tube photoreactor with a cylindrical configuration. The irradiation was provided by a 500 W halogen lamp which emitted irradiation comparable to sunlight. The distance between the surface of reaction solution and light source is adjusted to about 15 cm and the temperature of the photoreactor was controlled at 25±2 °C by continuous cooling water. A certain amount of photocatalyst powder (20 mg) is added to 120 ml aqueous Rhodamine-B (1.0×10^{-5} mol/L) solution. Before the occurrence of the photocatalytic degradation, the suspension is magnetically stirred in the dark for about 30 min to establish a Rhodamine-B adsorption-desorption equilibrium on catalyst surface as a reference point. The photocatalytic decomposition of RhB aqueous solution was characterized by a UV-visible spectrometer based on the Beer-Lambert law. During the irradiation experiments, aliquots (3 ml) are withdrawn from the suspension at regular time intervals and are immediately centrifuged at 5000 rpm for 10 min to remove solids. The concentration of Rhodamine-B after illumination is monitored at λ=553 nm using UV-vis spectrophotometer (Spectrumlab 2450, Shimadzu Corporation). The degradation rate of the Rhodamine-B can be determined by the formula: $X\%=(B_0-B_t)/B_0$, where B_0, B_t represents the initial absorbance and the absorbance after at time t of the aqueous RhB, respectively.

RESULTS AND DISCUSSION

Powder X-ray diffraction (PXRD) patterns were used to investigate the impact of gold modification on the phase structure and the chemical composition of Au-deposited TiO_2 nanoparticles and these factors have a great influence on its photocatalytic activity. For instance, many studies have confirmed that anatase form of titania exhibits a higher photocatalytic activity than brookite or rutile phase among the three main polymorphs. XRD profiles of Au-deposited TiO_2 and pure TiO_2 samples are depicted in Figure 1. It can be seen that the exclusively tetragonal anatase phase (International Center for Diffraction Data, JCPDS No. 71-1169, space group: I41/

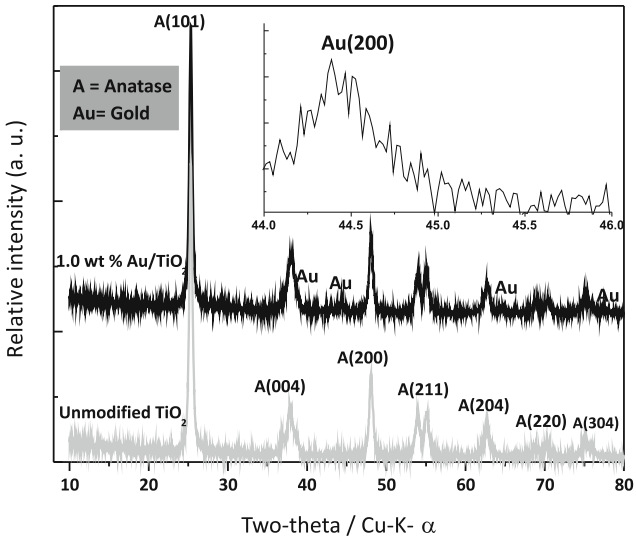

Figure 1. The wide-angle XRD patterns of (a) bare TiO_2 and (b) Au/TiO_2 photocatalysts

amd (141)) is identified for TiO_2 and Au/TiO_2 nanocomposite catalysts. The diffraction peaks at around 2Θ of 25.26, 37.89, 47.88, 53.98, 55.19, 62.75, 68.81, 70.15 and 75.02°represent the Miller indices of (101), (004), (200), (105), (211), (204), (116), (220) and (304) planes, respectively. Usually, the phase transformation temperature of amorphous to anatase of TiO_2 is around 400°C. Hence, it can be concluded that the phase transformation from amorphous to anatase is promoted to some degree in the present case. The well-defined diffraction pattern indicated that the as-synthesized product was already well crystallized. The addition of noble metals did not alter the crystalline phase composition of the TiO_2. None of the positions of the peaks changed significantly after deposition, which implies that there was no distortion of the original TiO_2 structure. Further observation shows that XRD peaks corresponding to Au/TiO_2 nanocomposite catalyst exhibit relatively weaker peak intensities and broader diffraction peak widths. The average crystallite sizes of TiO_2 and Au/TiO_2 nanocomposite catalysts can be estimated from the main diffraction peaks (101) using the Scherrer equation, $S=K\lambda/b\cos\Theta$, where the constant K is the shape factor with the value of 0.89, S is the crystal size, λ is the wavelength of X-rays (1.5408Å for Cu-kα radiation), Θ is the Bragg's angle, and b is the full width at half-maximum (fwhm) of the diffraction peak at Θ after subtraction of the instrument broadening. It was estimated that the average grain size is about 15.9 and 12.3 nm for bare TiO2 and Au/TiO_2 samples, respectively. It can be seen that the average crystallite sizes slightly decrease with Au modification, indicating that the gold presence influences crystallite size and the Au nanoparticles have a negative effect on the anatase grain growth, which is valid since the deposited Au nanoparticles suppress the growth of anatase nanocrystals by providing dissimilar boundaries and hinder the mass transportation. Distinction between gold and titania by XRD is not easy, especially in the case of fine titana particles as the peaks are broad and overlapped, and the peaks corresponding to the presence of Au are just above the noise level. However, several small peaks associated with the metal deposits were still observable in Fig. 1 (which should be enlarged due to the low Au content). The reflection at diffraction angle of $2\Theta=44.392^{o}$ can be assigned to the (200) plane of Au^0, which confirms the deposition of Au on the surface of titania. Compared to unmodified TiO_2 pattern, major peaks for Au/TiO_2 occur at the same 2Θ values for the former, suggesting that depositing of Au onto TiO_2 does not alter the crystal structure of Au/TiO_2. Furthermore, four peaks of Au at 2Θ values of 38.141, 44.392, 64.668 and 77.555° were observed for the Au/TiO_2 photocatalyst. The inset of Fig. 1 is an enlargement of the Au(200) peak for Au/TiO_2 sample, which confirms that Au deposition was responsible for new peak typical of crystalline gold, however, the peak corresponding to Au phase at $2\Theta=38.141^{o}$ is really hard to be seen and does not stand out of the background since this peak was just overlapped with that of titania at about 37.89° of (004) plane of anatase TiO_2. The as-prepared products were further characterized by TEM techniques to have an idea about the nanoparticle sizes and surface morphology affected during surface modification. As a representative example, the TEM image of the as-prepared Au–TiO_2 specimen was shown in Fig. 2. It can be seen that the gold particles exhibit sphere-like morphology and the structure of synthesized TiO_2 is irregular and ranged in size from 10 to 50 nm. The TEM permits easy differentiation of Au nanocrystals (small dark areas or dark spots) and TiO_2 crystallites (large bright areas). At first glance, a large number of spherical metal nanoparticles or clusters dispersed on the surface of TiO_2 were clearly observed as the darker spots and these spherical particles are fairly stable, well-defined and discrete, with a size of approximately 8–15 nm, even though this caused partial agglomeration to form block particles. The TEM technique also gives the evidence as to the presence of metallic Au with nano-size on the surface of titania particles.

To investigate the light absorption properties of the synthesized TiO_2 nanostructures and the effect of gold loading on their UV-vis light response, the UV-vis diffuse reflectance spectra including the absorption edge of TiO_2 and Au-deposited TiO_2 were determined using the absorption data in the range of 300–750 nm, from which the reflection was converted into absorbance by the Kubelka-Munk method and the results were portrayed in Fig. 3. It can be observed that the sample of bare TiO_2 has no obvious absorption in the visible region (> 400 nm) and the absorption edge of bare TiO_2 is ~380 nm

Figure 2. The TEM image of the as-prepared Au–TiO_2 composite material (1.0 wt % metal loadings)

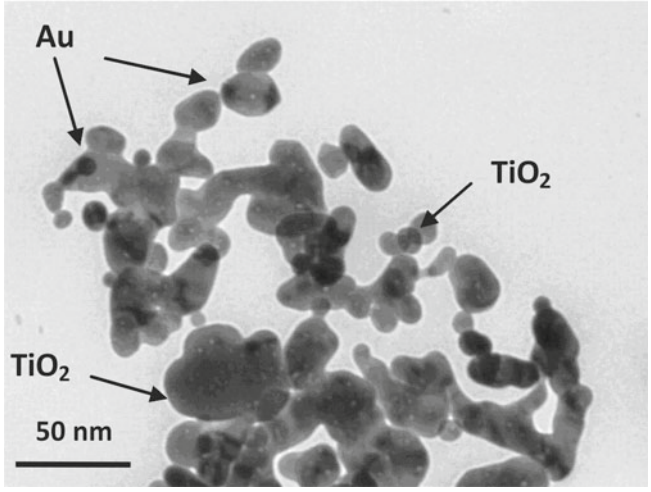

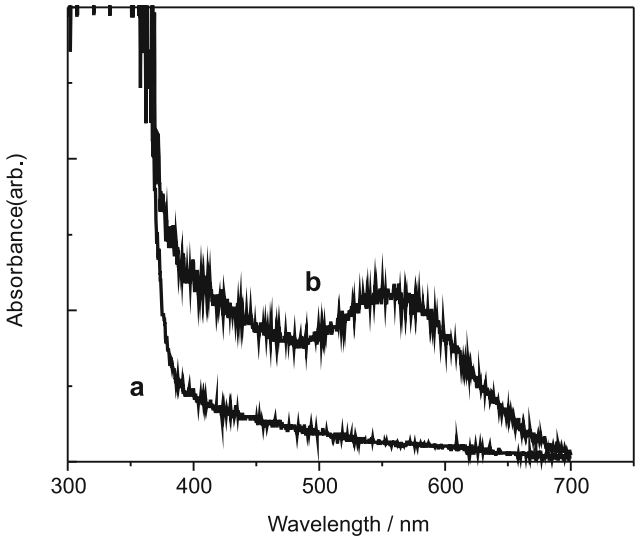

Figure 3. The optical absorption spectra of (a) bare TiO_2 and (b) Au/TiO_2 samples

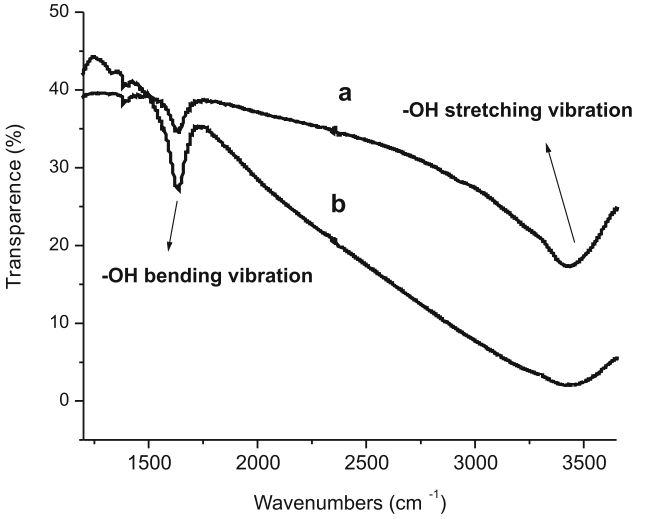

Figure 4. The Fourier transformation infrared spectra of (a) bare TiO_2 and (b) Au/TiO_2 nanoparticles

corresponding to the charge transfer from the valence band (mainly formed by 2p orbitals of the oxide anions) to the conduction band (mainly formed by 3d t_{2g} orbitals of the Ti^{4+} cations)[9], while the incorporation of metallic Au particles into TiO_2 exhibits an optical response in the visible region. In comparison with that of bare TiO_2, Au-deposited TiO_2 sample presents a substantial absorption red shift. In the visible part of the spectra the surface plasmon absorption effect due to gold nanoparticles can be observed with maxima around 560 nm. According to the relevant literatures[10], this absorbance band should be ascribed to the plasmon resonance of metallic Au nanoparticles coming from the collective oscillations of the free conduction-band electrons that are sparked by the incident electromagnetic radiation. It has been reported that the surface plasmon resonance of gold nanoparticles may be helpful to the separation of photogenerated charges created in the TiO_2, which could contribute to the enhancement of photocatalytic activity of composite catalyst studied here, and this is useful for fighting pollution with the sun light. Therefore, we could expect the improvement in the activity of the visible light-induced photocatalytic oxidation of organic pollutants.

The surface hydroxyl groups on titania have been recognized to play an important role on the photocatalytic reaction since they can inhibit the recombination of photogenerated charges and interact with photogenerated holes to product active oxygen species. Fig. 4 compares the IR transmittance spectra for the above considered TiO_2-based samples. FTIR spectra provide information on surface functional groups. As is shown, the bare TiO_2 and Au/TiO_2 samples exhibit similar infrared spectra spanning the range 1200–3650 cm^{-1}, and the broad and strong band around 3435 cm^{-1} which can be assigned to the γO-H stretching mode vibration of hydroxyl function groups (Ti-OH bonds). The other narrow and sharp peaks at 1631 cm^{-1} can be assigned to δO-H bending mode vibration of hydroxyl group on the surface of TiO_2 particles. This band signal increases in its intensity for Au/TiO_2 indicating the surface to be more hydroxylated compared to bare TiO_2. Therefore, the FTIR investigation confirms that pure titania has the lowest surface OH group density. The large surface hydroxyl group density will lead to an enhancement of the photocatalytic activity. Because they can interact with photogenerated holes, which gives better charge transfer and inhibits the recombination of electron-hole pairs.

PL emission spectra can be used to examine the fate of the photoinduced electron and holes in a semiconductor, since PL emission results from the recombination of free charge carriers. A semiconductor is characterized by the electronic band structure in which the lowest unoccupied molecular orbital (LUMO), called conduction band (CB), and the highest occupied molecular orbital (HOMO), called valence band (VB). The energy difference between the LUMO and HOMO level is viewed as band gap energy. For nanostructured materials, the PL spectra are related to the transfer behavior of the photogenerated electron and holes so that it can reflect the separation and recombination of photoformed charge carriers and it is employed to primarily evaluate the recombination probability of charge carriers. In general, a lower PL intensity might indicate a lower recombination rate of photo-generated electrons and holes[11]. As shown in Fig. 5, the PL intensity of TiO_2 was substantially quenched by the depositing with Au, indicating that the Au depositing

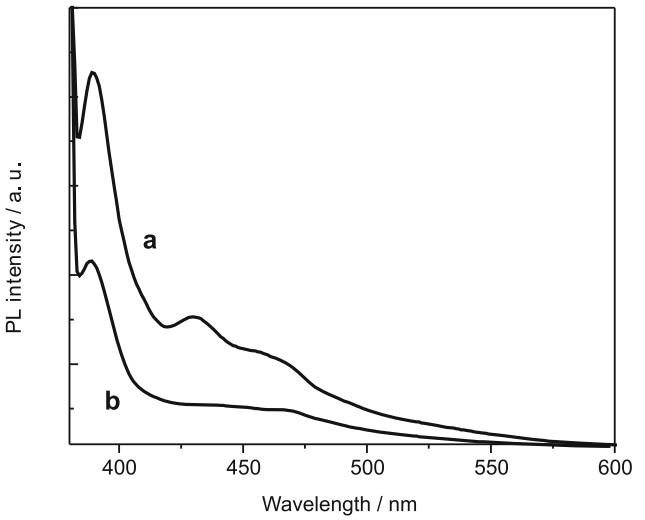

Figure 5. The PL spectra of (a) bare TiO_2 and (b) Au/TiO_2 photocatalysts (λ_{Ex}=320 nm)

suppresses the recombination of electron–hole pairs in TiO_2. This is ascribed to the fact that the electrons are excited from the valence band to the conduction band and then migrate to Au nanoparticles, which prevents the direct recombination of electrons and holes. This improved transport property of charge carriers on a semiconductor is expected to decrease the electron-hole recombination and promote the electron-hole separation. The noble metal Au deposited on TiO_2 act as electron traps, facilitating electron-hole separation and promoting the interfacial electron transfer process, which can bring high photon utilization efficiency and thus improve the photocatalytic activity of the catalyst.

The photocatalytic efficiency of the Au/TiO_2 nanostructured material is evaluated by conducting photooxidation experiments based on the decomposition of RhB dye. This toxic organic substance is used in the textile industry and it is harmful to the aquatic environment. For comparison, we conducted the same photocatalytic reactions with bare TiO_2. The absorption band of RhB dye was found to be centered at 553 nm. However, under dark conditions without light illumination, the concentration of RhB almost does not change for every measurement using as-prepared catalysts. Moreover, illumination in the absence of TiO_2 samples does not result in the photocatalytic decomposition of RhB. Therefore, the presence of both UV-vis illumination and TiO_2 samples is necessary for the efficient degradation. These results also suggest that the decomposition of RhB is caused by the photocatalytic reactions occurred on TiO_2 samples under the UV-vis illumination. After irradiation with UV-vis light source, the absorption intensity decreased due to the discoloration of RhB dye. Fig. 6 shows the removal of chemical pollution from the water and plots the concentration change of RhB as a function of irradiation time of different samples. The inset of Fig. 6 also shows the temporal evolution of the UV-vis absorption spectrum changes during the photocatalytic degradation of RhB in the UV-vis/TiO_2 process using Au/TiO_2 as a catalyst. As can be seen, the absorption peak corresponding to the RhB molecules at 553 nm rapidly decreased in intensity with exposure time. The absorption spectra reveal no evidence of the existence of new intermediates

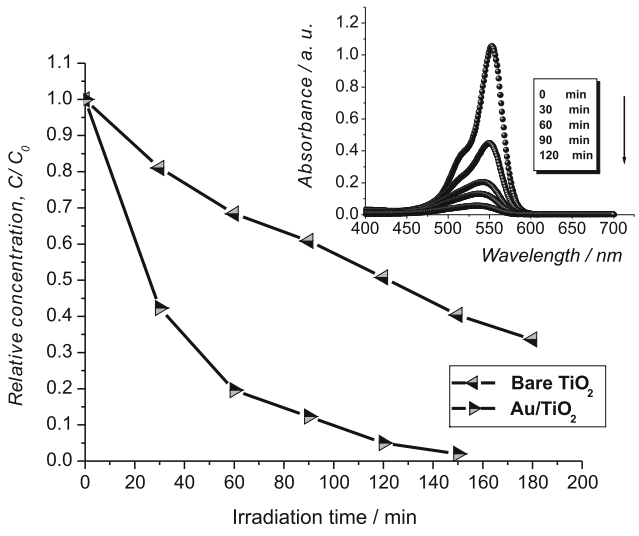

Figure 6. The kinetic curves of the photocatalytic removal of RhB dye for bare TiO_2 and Au/TiO_2 photocatalysts in the presence of UV-vis light excitation, respectively

or products formed in the visible region. Moreover, the maximum absorption peaks at 553 nm corresponding to RhB decreases considerably throughout the irradiation time and shifts also to shorter wavelengths (from 553.8 to 538.7 nm), according to the N-de-ethylation mechanism that the dye RhB is de-ethylated in a stepwise manner, and ethyl groups are removed one by one as confirmed by the gradual peak wavelength shifts toward the blue region[12]. As exposure time beyond 120 min, the original pink RhB dispersion turns almost completely into colorless solution, which implies that complete degradation of RhB was achieved. Of course, the peak blue shift could be ascribed to N-de-ethylation of RhB to rhodamine. By comparison, it was evident that the RhB degradation rate on Au/TiO_2 nanocomposite catalyst was faster than that on bare TiO_2 catalyst, which could be attributed to the following: (1) With the decreased particle sizes arising from gold deposition, the diffusion distances of the photogenerated holes from the bulk to the surface reaction sites shorten, engendering an increase in the number of holes reaching the reaction sites. (2) Upon UV-vis light activation, the effective separation of electron-hole pairs induced by Au nanoparticles results in an enhanced concentration of hydroxyl radicals on the surface of TiO_2 and thus leading to improved quantum efficiency for photochemical reaction system. (3) Photoinduced electrons can quickly transfer to the oxygen adsorbed on the surface of TiO_2, and these electrons can react with adsorbed molecular oxygen yielding superoxide anion radicals ($\cdot O2^-$). The superoxide anion radicals act as oxidizing agents or as an additional source of hydroxyl radicals. (4) The amount of the surface hydroxyl is increased, and holes can react with surface hydroxyl ions or water to produce hydroxyl radicals ($\cdot OH$), which are strong oxidizing species to react with RhB molecules and thus leads to the destruction of RhB. (5) The response range to light can be expanded to the visible region, which implies that Au-deposited TiO_2 catalyst can be activated by visible light and generate more photoinduced electrons and holes to participate the reaction. These advantages of the Au/TiO_2 photocatalysat remarkably improve its photocatalytic performance. In conclusion, the consequence of Au deposition is the improved photocatalytic activity under UV-vis light irradiation, though the relevant photocatalytic mechanisms can be quite different. Under UV-light irradiation, almost all semiconductor photocatalysts show an electronic transfer from valence band (VB) to conduction band (CB), leaving holes in the valence band. Then some of these photoinduced electrons or holes would migrate to the surfaces to participate in the photocatalytic reactions. Moreover, the photocatalytic mechanism upon Au deposition under visible-light irradiation can be described as follows. That is, Au nanoparticles were first excited under visible-light irradiation because the surface plasmon responsiveness occurred when receiving a continuous energy supply. Then excited electrons may transfer from the full band of Au below the Fermi level to its higher energy level. These activated electrons at higher energy levels may facilitate to migrate from Au to the CB of TiO_2 nanoparticles. Subsequently, electrons accepted by CB of TiO_2 nanoparticles could be directly captured by adsorbing the O_2 molecules in the vicinity of surfaces to

form the $O2^{-\bullet}$ species for the photocatalytic reactions. It should be mentioned that the time for producing the photoexcited electrons is much shorter than that for the reaction to form the $O2^{-\bullet}$ species and furthermore to decompose RhB molecules.

For a heterogeneous photocatalytic system, in principle, the reaction presumably takes place over the catalyst surface. Therefore, reactant adsorption on catalyst surface is regarded as a pre-requisite step and the photodegradation reaction is a synergistic process. Photocatalytic degradation can be represented as $R = R_1 + R_2$, where R, R_1 and R_2 are net degradation, photocatalysis and photolysis rates, respectively. Under chosen experimental conditions, photolysis had no effect on degradation process. Therefore, the net degradation rate amounts to the photocatalysis rate. For the correct evaluation of kinetic data for disappearance of water pollutants we applied the Langmuir-Hinshelwood model using the rate equation for heterogeneous photocatalytic reactions[13]:

$$\frac{1}{R} = -\frac{dt}{dC} = \frac{1}{kK} \times \frac{1}{C} + \frac{1}{k} \quad (1)$$

where R is the reaction rate, k is reaction rate constant, K is the adsorption coefficient of the reactant of Langmuir's isotherm, and C is the reactant concentration. The values of k and K are used to explain the coefficients defining the rate determining reaction events and pre-equilibrium adsorption within an adsorbed monolayer at the oxide material surface and the aqueous solution interface. The effect of light intensity is also incorporated in k and K which accounts for the equilibrium constant for fast adsorption-desorption processes between surface monolayer and bulk solution[14]. After integration of the above formula it is transformed to:

$$t = \frac{1}{kK} \ln[C_0 / C] + \frac{1}{k}(C_0 - C) \quad (2)$$

if the solution is highly diluted or C is very small especially as the initial concentration (C_0) of RhB dye is a millimolar solution (C_0«0.1 mmol L^{-1}), and in this case K·C[RhB]«1or the KC product is negligible with respect to unit so that the reaction follows apparent first-order kinetics according to Equation (3):

$$-ln(\frac{C}{C_0}) \approx kKt = k_{app}t \quad (3)$$

where C_0 is the dye concentration of the initial one and kapp is the apparent first-order reaction constant representing the reaction rate R (with the same restriction of $C=C_0$ at t=0, with t being the reaction time). In this case, the photocatalytic degradation process will follow an ideal pseudo-first-order behavior, and the pseudo-first-order rate constant was chosen as the basic kinetic parameter to compare photoreactivity of different catalysts since it is not related to the adsorbed dye concentration and thus it is possible to determine the photocatalytic efficiency independent of previous adsorption period in the dark. To obtain a quantitative understanding on the bleaching reaction kinetics of the RhB degradation, we thus applied the pseudo-first order model as expressed by equation $\ln(C_0/C) = -kapp \cdot t$, and the curves of $\ln(C_0/C)$ against t were recorded and fitted linearly and the slope of the fitted line representing kapp was extracted and compared. Using this method, the values of k_{app} (apparent reactivity) for the different catalysts (bare TiO_2 and Au/TiO_2 samples) in the decomposition of RhB dye can be estimated from a graph of $[\ln(C_0/C)]$ against t. As can be seen, the plot of $\ln(C_0/C)$ vs. irradiation time yields a linear relationship (Fig. 7) indicating a very good simulation (confidence coefficient $R>0.99$) using the first-order dynamics. The pseudo-first order rate constants of the reactions in the presence of Au/TiO_2 (kAu/TiO_2), TiO_2 ($kTiO_2$) and magnitude of these values are 0.0252 min^{-1} and 0.0059 min^{-1}, respectively. Clearly, the Au/TiO_2 nanocomposite catalyst showed a better photocatalytic activity than the bare TiO_2 catalyst. The discrepancy between the pseudofirst-order reaction rate constants is that the photocatalytic degradation process involves a complicated mechanism which would be influenced by many factors such as particle size, phase/chemical composition, surface properties, effectiveness of charge separation and therefore in the efficiency of photocatalysis as discussed above. The result confirms that reaction rate of photodegradation of RhB dye and photocatalytic activity could be achieved by incorporating TiO_2 with metallic gold nanoparticles.

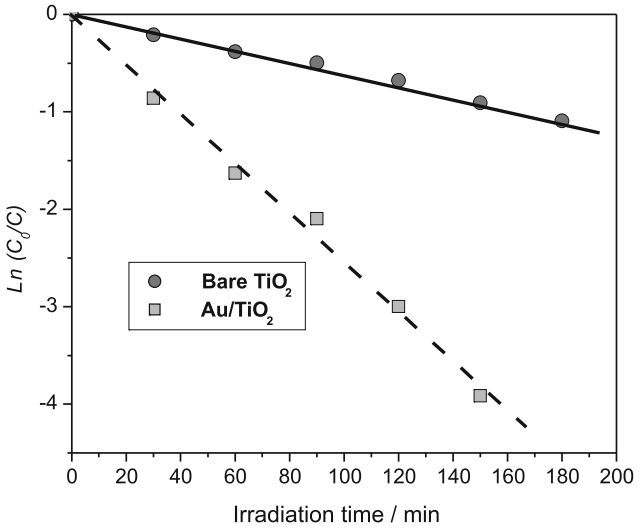

Figure 7. Variation in $\ln(C_0/C)$ as a function of irradiation time and linear fits of bare TiO_2 and Au/TiO_2 photocatalysts, respectively

CONCLUSIONS

In summary, a high efficient Au-loaded TiO_2 nanophotocatalyst was synthesized through the chemical reduction using hydrazine hydrate as the reducing agent. The photocatalytic activity and the corresponding kinetics of the as-prepared catalyst under UV-vis light excitation were examined by using the removal of RhB aqueous solution as a test reaction. The results suggest that the recombination of the photoinduced charge carriers can be largely restrained by Au modification and the Au-loaded TiO_2 photocatalyst possess higher surface hydroxyl group density. The photocatalytic activity of Au/TiO_2 nanocomposite is improved remarkably compared to that of bare TiO_2. The enhanced photocatalytic performance was ascribed to the promotion of charge separation, increasing of OH group density and the extension of the optical response of catalyst into the visible range. Moreover, degradation kinetics of RhB dye can be well described by Langmuir-Hinshelwood model. The photocatalytic removal of RhB dye by Au/TiO_2 photocatalyst can be viewed as a practical and useful way for the removal of

environmental pollutants and is expected to expand its potential application in sewage water treatment.

ACKNOWLEDGMENTS

This work was supported by Hubei Provincial Natural Science Foundation of China (Project no. 2011CDB148).

LITERATURE CITED

1. Li, Q., Mahendra, S., Lyon, D., Brunet, L., Liga, M., Li, D. & Alvarez, P. (2008). Antimicrobial nanomaterials for water disinfection and microbial control: potential applications and implications. *Water. Res*. 42, 4591–4602. DOI: 10.1016/j.Watres.2008.08.015.

2. Tryba, B., Brożek, P., Piszcz, M. & Morawski, A.W. (2011). New photocatalyst for decomposition of humic acids in photocatalysis and photo-Fenton processes. *Pol. J. Chem. Tech*. 13(4), 8–14. DOI: 10.2478/v10026-011-0042-5.

3. Li, X., Wang, L. & Lu, X. (2010). Preparation of silver--modified TiO_2 via microwave-assisted method and its photocatalytic activity for toluene degradation. *J. Hazard. Mater*. 177, 639–647. DOI: 10.1016/j.jhazmat.2009.12.080.

4. Chan, S. & Barteau, M. (2005). Preparation of Highly Uniform Ag/TiO_2 and Au/TiO_2 Supported Nanoparticle Catalysts by Photodeposition. *Langmuir*. 21(12), 5588–5595. DOI: 10.1021/la046887k.

5. Hou, L.R., Yuan, C.Z. & Peng, Y. (2007). Synthesis and photocatalytic property of SnO_2/TiO_2 nanotubes composites. *J. Hazard. Mater.* 139, 310–315. DOI: 10.1016/j.jhazmat.2006.06.035.

6. Li, J. & Zeng, H.C. (2006). Preparation of Monodisperse Au/TiO_2 Nanocatalysts via Self-Assembly. *Chem. Mater.* 18(18), 4270–4277. DOI: 10.1021/cm060362r.

7. Li, H., Bian, Z., Zhu, J., Huo, Y., Li, H. & Lu, Y. (2007). Mesoporous Au/TiO_2 Nanocomposites with Enhanced Photocatalytic Activity. *J. Am. Chem. Soc*. 129(15), 4538–4539. DOI: 10.1021/ja069113u.

8. Jain, R., Mathur, M., Sikarwar, S. & Mittal, A. (2007). Removal of the hazardous dye Rhodamine B from photocatalytic and adsorption treatments. *J. Environ. Manag*. 85, 956–964. 10.1016/j.jenvman.2006.11.002.

9. Zhang, X.T., Zhou, G.W., Zhang, H.Y., Wu, C.C. & Song, H.B. (2011). Characterization and activity of visible light–driven TiO_2 photocatalysts co-doped with nitrogen and lanthanum. *Transition. Met. Chem*. 36, 217–222. DOI: 10.1007/s11243-010-9457-8.

10. Yusuke, I., Mizuki, M. & Makoto. O. (2010). Efficient Visible-Light-Induced Photocatalytic Activity on Gold-Nanoparticle-Supported Layered Titanate. *J. Am. Chem. Soc*. 132(47), 16762–16764. DOI: 10.1021/ja1083514.

11. Li, F.B. & Li, X.Z. (2002). The enhancement of photodegradation efficiency using $Pt–TiO_2$ catalyst. *Chemosphere*. 48(10), 1103–1111. DOI: 10.1016/S0045-6535(02)00201-1.

12. Zhong, H.E., Yang, S.G., Ju, Y.M. & Sun. C. (2009). Microwave photocatalytic degradation of Rhodamine B using TiO2 supported on activated carbon: Mechanism implication. *J. Environ. SCi*. 21(2), 268–272. DOI: 10.1016/S1001-0742(08)62262-7.

13. Pedro, J.S., Valente, S., Padilha, P.M. & Florentino, A.O. (2006). Studies in the adsorption and kinetics of photodegradation of a model compound for heterogeneous photocatalysis onto TiO_2. *Chemosphere*. 64(7), 1128–1133. DOI: 10.1016/j.chemosphere.2005.11.050.

14. Tsunoyama, H., Ichikuni, N. & Tsukuda, T. (2008). Microfluidic Synthesis and Catalytic Application of PVP-Stabilized, ~1 nm Gold Clusters. *Langmuir*. 24(20), 11327–11330. DOI: 10.1021/la801372j.